Carbon–Carbon Bond Formation via Carbyne–Carbonyl Migratory Coupling Promoted by H^- or OR^- Addition to $[Fe_2(\mu\text{-CSR})(\mu\text{-CO})(CO)_2(Cp)_2]^+$

Luigi Busetto,*,† Valerio Zanotti,† Luca Norfo,† Antonio Palazzi,† Vincenzo G. Albano,‡ and Dario Braga*,‡

Dipartimento di Chimica Fisica ed Inorganica, Università di Bologna, Viale Risorgimento 4, 40136 Bologna, Italy, and Dipartimento di Chimica "G. Ciamician", Università di Bologna, Via Selmi 2, 40126 Bologna, Italy

Received July 6, 1992

The complexes $[Fe_2(\mu\text{-CSR})(\mu\text{-CO})(CO)_2(Cp)_2]^+$ [R = Me (**1a**), Et (**1b**)] react with $LiHBEt_3$ to form $FeFe[\mu\text{-C(CHO)SR}](\mu\text{-CO})(CO)(Cp)_2$ (**2a,b**), together with smaller amounts of $Fe_2[\mu\text{-C(CHO)H}](\mu\text{-CO})(CO)(Cp)_2$ (**3**). The major product, the aldehyde **2**, is proposed to result from H^- addition at the terminally coordinated CO ligand in **1** and subsequent CHO migration to the bridging carbyne carbon atom. The corresponding reactions of **1a,b** with RO^- (R = Me, Et) afford the alkoxycarbonyls $Fe_2(\mu\text{-CSR})(\mu\text{-CO})(CO)(COOR')(Cp)_2$ (**4**), which in turn, upon standing in CH_2Cl_2 solution, rearrange to form the esters $FeFe[\mu\text{-C(COOR')SR}](\mu\text{-CO})(CO)(Cp)_2$ (**5**). The relevance of these reactions is discussed in the general context of C–C bond formation involving transition metal complexes. In addition to spectroscopic characterization three compounds [**2b**, **3**, **5a** (R = R' = Me)] have been fully characterized by X-ray crystallography. These molecules contain the bonded Fe–Fe unit supporting a bridging CO and a bridging carbene unit. The sulfur atom is also coordinated to the iron in **2a** and **5a**, in the place of a terminal CO ligand. The carbene atoms bear a CHO substituent in **2b** and **3** and a C(O)OMe substituent in **5a**. The $\eta\text{-}C_5H_5$ groups occupy mutually cis coordination sites.

Introduction

The chemistry of dinuclear complexes containing bridging carbyne ligands has received much attention in recent years. In this class of compounds the thiocarbyne derivatives $[Fe_2(\mu\text{-CSR})(\mu\text{-CO})(CO)_2(Cp)_2]^+$ (**1**) have been extensively studied demonstrating that their reactivity is dominated by the electrophilic character of the μ-carbyne carbon which easily undergoes addition by a variety of nucleophiles such as RS^- (R = Me, Ph, Bz), $PhSe^-$, BH_4^-,[1] and CN^- [2] to give the corresponding carbene derivatives. On the other hand, we have recently reported that the NCO^- insertion reaction into the μ-C–S bond occurs with formation of the isocyanide complexes $Fe_2[\mu\text{-CNC(O)SR}](\mu\text{-CO})(CO)_2(Cp)_2$.[3] Another example of reaction involving the thiocarbyne function is that of **1** with $NaCo(CO)_4$ resulting in the formation of a triply bridging carbyne cluster.[4]

However other reactive centers are present in **1** and Quick and Angelici have shown that CO substitution reactions take place with phosphines, phosphites, isocyanides, and halides that give $[Fe_2(\mu\text{-CSR})(\mu\text{-CO})(L)(CO)(Cp)_2]^+$.[5] In view of the fact that the carbon atom of the CO groups in cationic metal carbonyls can undergo facile attack by nucleophiles, one should expect that **1** might also be involved in analogous reactions. Herein we report the reactions of the μ-thiocarbonyl cations $[Fe_2(\mu\text{-CSR})(\mu\text{-CO})(CO)_2(Cp)_2]^+$ (**1**) with $LiHBEt_3$ and alkoxides RO^- (R = Me, Et) resulting in the formation of formyl and alkoxycarbonyl ligands which subsequently migrate to the μ-carbyne carbon.

Results

Reactions of $Fe_2(\mu\text{-CSR})(\mu\text{-CO})(CO)_2(Cp)_2$ [R = Me (1a), Et (1b)] with $LiHBEt_3$. When a red solution of **1** in tetrahydrofuran (THF) was mixed with 1 equiv of lithium triethylborohydride under argon atmosphere at −60 °C, it immediately turned green. An IR inspection of the reaction mixture showed that the characteristic carbonyl absorptions due to *cis*-**1** were completely replaced by a different set at lower energy. Thin-layer chromatographic examination of the crude reaction mixture revealed the presence of three products with a large predominance of the second moving component. Separation by column chromatography of the faster-moving fraction provided a solution containing small amounts of $[Fe(CO)_2(Cp)]_2$. The second component **2** was obtained as a dark-green crystalline solid (about 65% yield) and has been studied by X-ray diffraction on **2b** (see later). The infrared spectra of **2** contain bands due to the single terminal and bridging carbonyl ligands at 1958 (s) and 1782 (ms) cm^{-1} (CH_2Cl_2)

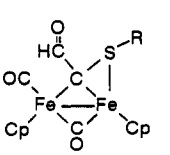

2a, R = Me; 2b, R = Et

† Dipartimento di Chimica Fisica ed Inorganica.
‡ Dipartimento di Chimica "G. Ciamician".

(1) Schroeder, N. C.; Funchess, R.; Jacobson, R. A.; Angelici, R. J. *Organometallics* **1989**, *8*, 521.
(2) Busetto, L.; Bordoni, S.; Zanotti, V.; Albano, V. G.; Braga, D. *Gazz. Chim. Ital.* **1988**, *118*, 667.
(3) Busetto, L.; Carlucci, L.; Zanotti, V.; Albano, V. G.; Braga, D. *J. Chem. Soc., Dalton Trans.* **1990**, 243.
(4) Schroeder, N. C.; Richardson, J. W.; Wang, S. L.; Jacobson, R. A.; Angelici, R. J. *Organometallics* **1985**, 4, 1226.
(5) Quick, M. H.; Angelici, R. J. *Inorg. Chem.* **1981**, *20*, 1123.

0276-7333/93/2312-0190$04.00/0

as well as a band at 1619 (m) cm^{-1} assigned to the carbonyl of the CHO group. The position of the first two bands is strictly comparable to that found in $FeFe[\mu\text{-}C(CN)SR](\mu\text{-}CO)(CO)(Cp)_2$[2] (1959, 1783 cm^{-1}) and in $FeFe[\mu\text{-}C(CN)OCH_2CH{=}CH_2](\mu\text{-}CO)(CO)(Cp)_2$[6] (1958, 1787 cm^{-1}), where the bridging ligands are also doubly coordinated to the iron atoms. Furthermore the presence of C(SR)CHO is indicated by the observation in the ^{13}C NMR spectrum of signals for the μ-C and CHO carbons at δ 161.7 and 199.9, respectively. The ^1H NMR spectra of **2a,b** show signals for the aldehyde protons at about δ 11.6 and upfield-shifted resonances for the SR protons (δ 1.73 for **2a**), which is typical for a mercaptide group S-coordinated to a metal center. The slower-moving component **3** was isolated as a red crystalline solid (5% yield). Its nature has been ascertained by an X-ray study (see later). The spectroscopic properties (IR and NMR) of **3** are identical to those reported by Casey et al., who first prepared the complex **3**.[7]

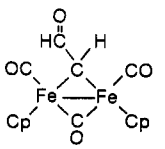

3

Reactions of $Fe_2(\mu\text{-}CSR)(\mu\text{-}CO)(CO)_2(Cp)_2$ (1a,b) with Alkoxides. Addition of equimolar amounts of RO^- (R = Me, Et) to a THF solution of **1a,b** at −20 °C, followed by warming at room temperature, results in a color change from deep red to green with formation of $Fe_2(\mu\text{-}CSR)(\mu\text{-}CO)(CO)(COOR')(Cp)_2$ (**4a–c**) (**4a**, R = R′ = Me; **4b**, R = Me, R′ = Et; **4c**, R = R′ = Et) in about 50–60% yield.

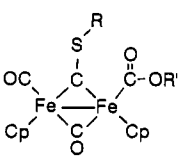

4a-c

Type **4** complexes are air sensitive and decompose on standing in CH_2Cl_2 solution, at room temperature, after 24 h. Chromatography of the decomposition mixture gives small amounts of $[Fe(\mu\text{-}CO)(CO)(Cp)]_2$ together with $Fe_2(\mu\text{-}CS)(\mu\text{-}CO)(CO)_2(Cp)_2$ as a first reddish-brown fraction. A second green fraction gives, after evaporation of the solvent and crystallization from CH_2Cl_2–pentane, green crystals of $FeFe[\mu\text{-}C(COOR')SR](\mu\text{-}CO)(CO)(Cp)_2$ (**5a–c**) (**5a**, R = R′ = Me; **5b**, R = Me, R′ = Et; **5c**, R = R′ = Et) in about 20% yield.

While the nature of **5** has been unequivocally ascertained by a X-ray diffraction study on **5a**, type **4** complexes have been characterized on the basis of their spectroscopic features. Their infrared spectra show bands attributable to the single terminal and bridging carbonyl ligands (1984 and 1805 cm^{-1} for **4a**) and a band at about 1614 cm^{-1} assigned to the metal-bonded alkoxycarbonyl group. In

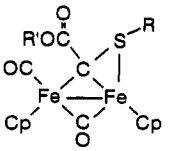

5a, R = R'= Me;
5b, R = Me, R' = Et;
5c, R = R'= Et

the ^1H NMR spectra strong sharp singlets are observed for the two unequivalent Cp ligands (δ 4.81, 4.79 for **4a**). The instability of type **4** complexes prevented satisfactory ^{13}C NMR characterization. However the spectrum of **4a**, recorded at −60 °C, showed a resonance at δ 395.5 (CD_2Cl_2) which is in the typical range of bridging thiocarbyne carbons.[8] Other resonances were observed at δ 203.7 (COOR), 213.1 (CO), and 265.1 (μ-CO). Type **5** complexes exhibit, in their IR spectra, a ν(CO) band pattern analogous to that of the related type **2** complexes. It consists of two bands at 1949 and 1775 cm^{-1} assigned to the terminal and bridging CO ligands, respectively, together with a band at 1675 cm^{-1}, due to the COOR group, which is shifted to higher frequencies compared to that observed in the spectrum of **4** indicating that the carboalkoxy group is bonded to a carbon atom. The ^{13}C NMR spectrum of **5b** shows resonances at δ 155.7 and 180.0 attributable to the bridging alkylidene carbon and the carbonyl of the COOR group, respectively. As it has been observed for $FeFe[\mu\text{-}C(CHO)SR](\mu\text{-}CO)(CO)(Cp)_2$ (**2a,b**), the ^1H NMR spectra of **5** exhibit upfield resonances for the SR protons (δ 1.57 for SMe in **5a**) compared to those of the parent compound **4** (δ 3.41 in **4a**). This shift is indicative of the double-bridging coordination mode of the μ-C(COOR′)-SR ligand.

X-ray Molecular Structures of $FeFe[\mu\text{-}C(CHO)SEt](\mu\text{-}CO)(CO)(Cp)_2$ (2b), $Fe_2[\mu\text{-}C(CHO)H](\mu\text{-}CO)(CO)_2(Cp)_2$ (3), and $FeFe[\mu\text{-}C(COOR')SR](\mu\text{-}CO)(CO)(Cp)_2$ (5a). The molecular structures of **2b**, **3**, and **5a** are closely related. The three molecules are represented in Figures 1–3 together with the atomic labeling schemes. Complexes **3** and **5a** have two chemically equivalent independent molecules in the respective unit cells (see Experimental Section), and their relevant structural parameters are listed together in Tables II and III. Table I reports bond distances and angles for the species **2b**. The molecules **2b** and **5a** are chiral and the crystals contain racemic mixtures, while **3** conforms to an idealized C_s symmetry. The three complexes contain the same skeleton, namely a dimeric Fe_2 unit that supports two cis C_5H_5 ligands and one bridging CO ligand. The Fe–Fe bonds have strictly comparable lengths: 2.524 (1) in **2b**, 2.500 (1) and 2.540 (1) in **5a**, and 2.527 (1) and 2.523 (1) Å in **3**. It is noteworthy that the largest difference in the Fe–Fe bond distance is exhibited by the two independent values of **5a** clearly showing the relevance of the packing forces in influencing the softer bond interactions. The differences among the three species arise from the nature and mode of bonding of the carbene units. The C(carbene) atom in **2b** and **5a** is linked to an SEt and SMe unit, respectively, and the sulfur atom is bound to the Fe atom without terminal CO. The S–Fe and S–C(carbene)

(6) Busetto, L.; Cassani, M. C.; Zanotti, V.; Braga, D.; Albano, V. G. *J. Organomet. Chem.* **1991**, *415*, 395.
(7) Casey, C. P.; Crocker, M.; Niccolai, G. P.; Fagan, P. J.; Konings, M. S. *J. Am. Chem. Soc.* **1988**, *110*, 6070.
(8) Broadhurst, P. V. *Polyhedron* **1985**, *12*, 1801.

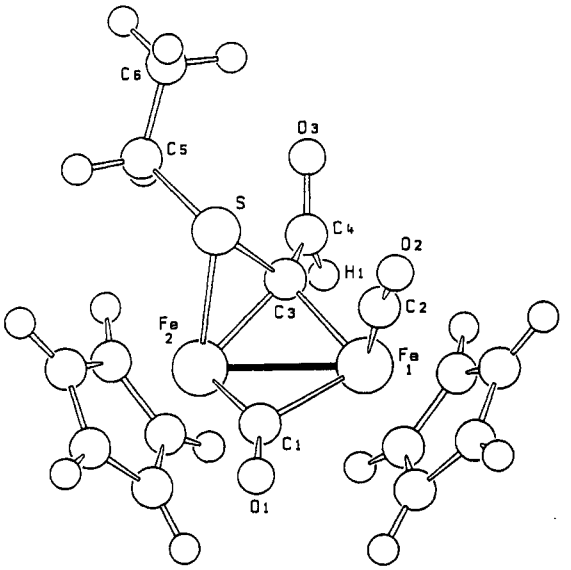

Figure 1. Molecular structure of **2b**, showing the atomic labeling scheme.

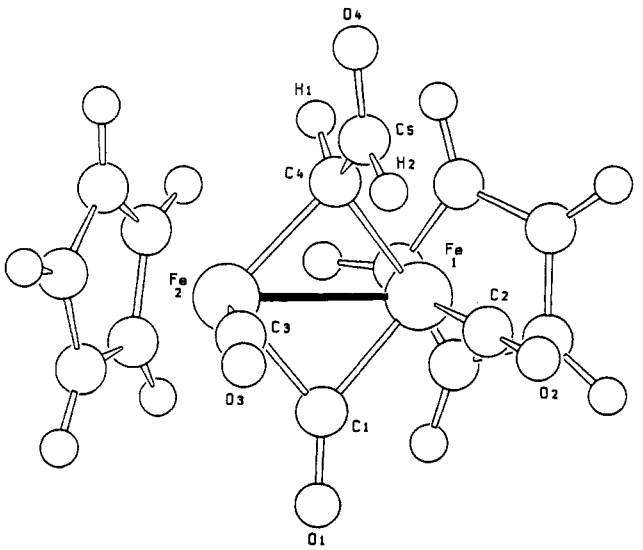

Figure 2. Molecular structure of **3**, showing the atomic labeling scheme. (Only one of the two independent molecules is shown.)

bond distances are strictly comparable in the two species [2.273 (1) and 2.269 (1), 2.268 (1) Å in **2b**; 1.771 (1) and 1.777 (5), 1.771 (5) Å in **5a**]. The C(carbene) atom bears a CHO group in **2b** and a C(O)OMe group in **5a** (see Figures 1 and 2). In **3** the carbene atom is bound to an H atom and to a CHO group (see Figure 3). In spite of the structural differences the bond distances around the carbene atoms are not substantially affected. Since the H atoms in **3** were located directly from the Fourier maps (see Experimental Section), it is possible to comment on the H–C(carbene)–C(formyl) and on O(4)–C(formyl)–H(formyl) bond angles [106 (2), 111 (3) and 115 (2), 120 (3)°, respectively]. While the latter values better conform to the sp^2 hybridization of the C(formyl) atom, the angles at μ-C are appreciably smaller than 120°, reflecting significant repulsions with the electrons in the metallacycle ring.

The presence of the S–Fe bond for **2b** and **5a** affects the bond length distribution within the bridging ligands. The Fe–C distances involving the Fe atom bound to sulfur are shorter than those involving the Fe atom bearing the

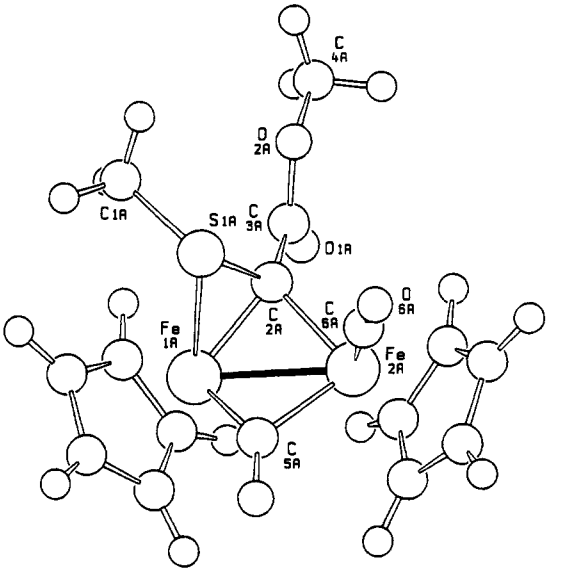

Figure 3. Molecular structure of **5a**, showing the atomic labeling scheme. (Only one of the two independent molecules is shown.)

terminal CO ligand [**2b**, Fe–C(μ-CO) = 1.843 (1) versus 2.030 (2) Å and Fe–C(carbene) = 1.910 (1) versus 1.965 (1) Å; **5a**, Fe–C(μ-CO) = 1.828 (5), 1.815 (5) versus 1.967 (6), 2.110 (5) Å and Fe–C(carbene) = 1.910 (5), 1.889 (5) versus 1.959 (5), 1.969 (5) Å]. As one can see, the effect is much more pronounced for the bridging CO ligand and can be explained in terms of lower π-accepting ability of the sulfur ligand, compensated by a stronger π bond to the bridging carbonyl.

Discussion

The formation of **2**, containing the CHO group bonded at the μ-carbene carbon, is rather surprising in light of the recently reported reaction of **1** with $NaBH_4$ by Angelici that, at room temperature, affords the μ-alkylidene $Fe_2[\mu\text{-C(SR)H}](\mu\text{-CO})(CO)_2(Cp)_2$.[1] The different result is partially explained by the fact that in most reactions involving metal carbonyls and hydride donors both the source of the hydride and the temperature are critical factors. Reductions with monohydrides such as $LiHBEt_3$ or trialkoxyborohydrides have been found particularly convenient in order to selectively obtain metal formyls,[9] while reductions with $NaBH_4$ or BH_3 are often accompanied by further reduction to hydroxomethyl or methyl complexes.[10] The reaction temperature is also important since in many cases formyl complexes have been isolated or simply detected by performing the reduction reactions at low temperature (lower than −50 °C).[11] Therefore, the reaction leading to the formation of **2** from **1** and $LiHBEt_3$ at −60 °C may be formally divided in two steps: (i) the well-documented hydride attack on the terminally coordinated CO group,[12] which forms the neutral thiocarbyne-bridged complex [**A**]; (ii) the unprecedented migration of

(9) (a) Casey, C. P.; Meszaros, M. W.; Neumann, S. M.; Cesa, I. G.; Haller, K. J. *Organometallics* **1985**, *4*, 143. (b) Casey, C. P.; Andrews, M. A.; McAlister, D. R.; Rinz, J. E. *J. Am. Chem. Soc.* **1980**, *102*, 1927. (c) Tam, W.; Marsi, M.; Gladysz, J. A. *Inorg. Chem.* **1983**, *22*, 1413. (d) Tam, W.; Lin, G. Y.; Gladysz, J. A. *Organometallics* **1982**, *1*, 525.

(10) Sweet, J. R.; Graham, W. A. G. *J. Am. Chem. Soc.* **1982**, *104*, 2811.

(11) (a) Gauntlett, J. T.; Mann, B. E.; Winter, M. J.; Woodward, S. *J. Chem. Soc., Dalton Trans.* **1991**, 1427. (b) Gauntlett, J. T.; Taylor, B. F.; Winter, M. J. *J. Chem. Soc., Dalton Trans.* **1985**, 1815.

(12) Gladysz, J. A. *Adv. Organomet. Chem.* **1982**, *20*, 1.

Table I. Crystal Data and Details of Measurements for 2b, 3, and 5a

	compd		
	2b	**3**	**5a**
M_r	400.06	367.93	416.04
cryst size (mm)	0.15 × 0.1 × 0.2	0.2 × 0.2 × 0.2	0.3 × 0.2 × 0.2
system	monoclinic	monoclinic	orthorhom
space group	$P2_1/c$	$P2_1/c$	$Pna2_1$
a (Å)	10.218 (2)	9.148 (2)	14.187 (1)
b (Å)	9.672 (1)	17.993 (3)	7.983 (1)
c (Å)	15.963 (3)	16.667 (3)	28.576 (15)
β (deg)	99.75 (2)	90.67 (2)	
U (Å^3)	1554.8	2743.2	3236.4
Z	4	8	8
F(000)	816	1488	1696
λ(Mo Kα) (Å)	0.710 69	0.710 69	0.710 69
μ(Mo Kα) (cm^{-1})	19.1	20.3	18.4
θ range (deg)	2.5–38	2.5–30	2.5–30
ω-scan width (deg)	0.9	0.75	0.7
requested counting $\sigma(I)/I$	0.01	0.01	0.01
prescan rate (deg min^{-1})	5	5	5
prescan acceptance $\sigma(I)/I$	0.5	0.5	0.5
max scan time (s)	150	120	120
range of reflcns measd ($h_{min}h_{max}$,$k_{min}k_{max}$,$l_{min}l_{max}$)[a]	±12,+10,+16	±8,+17,+16	+9,+16,+34
no. of measd reflcns	14 007	5112	3203
no. of unique obsd reflcns used in the refinement [$I_o > 2\sigma(I_o)$]	5356	3480	2581
no. of refined params	203	262	394
R, R_w[b]	0.028, 0.034	0.030, 0.034	0.031, 0.035
S	2.5	1.8	2.5
k, g[b]	1.0, 1.8 × 10^{-3}	2.3, 3 × 10^{-4}	2.2, 5 × 10^{-4}

[a] h_{min} = 0 in **5a**; k_{min} = l_{min} = 0 in **2b**, **3**, and **5a**. [b] $R_w = \sum[(|F_o| - |F_c|)w^{1/2}]/\sum|F_o|w^{1/2})$, where $w = k/[\sigma^2(F) + |g|F^2]$.

Table II. Relevant Bond Distances (Å) and Angles (deg) for 2b

Fe(1)–Fe(2)	2.524 (1)	C(7)–C(8)	1.398 (3)
Fe(2)–S	2.273 (1)	C(8)–C(9)	1.394 (3)
Fe(1)–C(1)	2.030 (2)	C(9)–C(10)	1.415 (4)
Fe(2)–C(1)	1.843 (1)	C(10)–C(11)	1.411 (3)
Fe(1)–C(2)	1.755 (2)	C(7)–C(11)	1.394 (3)
Fe(1)–C(3)	1.965 (1)	C(12)–C(13)	1.411 (3)
Fe(2)–C(3)	1.910 (1)	C(13)–C(14)	1.424 (3)
C(1)–O(1)	1.176 (2)	C(14)–C(15)	1.406 (3)
C(2)–O(2)	1.154 (2)	C(15)–C(16)	1.411 (3)
C(3)–C(4)	1.458 (2)	C(12)–C(16)	1.411 (3)
C(4)–O(3)	1.212 (3)		
C(4)–H(1)	1.080 (3)	Fe(1)–C(1)–O(1)	131.9 (1)
C(3)–S	1.771 (1)	Fe(2)–C(1)–O(1)	146.1 (1)
S–C(5)	1.823 (2)	Fe(1)–C(2)–O(2)	174.6 (2)
C(5)–C(6)	1.527 (3)	Fe(1)–C(3)–C(4)	122.3 (1)
Fe(1)–C(7)	2.140 (2)	Fe(2)–C(3)–C(4)	130.7 (1)
Fe(1)–C(8)	2.096 (2)	Fe(1)–C(1)–Fe(2)	81.2 (1)
Fe(1)–C(9)	2.076 (2)	Fe(1)–C(3)–Fe(2)	81.3 (1)
Fe(1)–C(10)	2.094 (2)	Fe(2)–S–C(5)	109.2 (1)
Fe(1)–C(11)	2.126 (2)	Fe(2)–S–C(3)	54.7 (1)
Fe(2)–C(12)	2.093 (2)	S–C(3)–C(4)	121.7 (1)
Fe(2)–C(13)	2.072 (2)	C(3)–C(4)–O(3)	126.6 (2)
Fe(2)–C(15)	2.106 (2)	C(3)–C(4)–H(1)	116.8 (2)
Fe(2)–C(16)	2.110 (2)	S–C(5)–C(6)	110.4 (1)

Table III. Relevant Bond Distances (Å) and Angles (deg) for 3

molecule 1		molecule 2	
		Distances	
Fe(1)–Fe(2)	2.527 (1)	Fe(3)–Fe(4)	2.523 (1)
Fe(1)–C(1)	1.907 (4)	Fe(3)–C(16)	1.915 (4)
Fe(2)–C(1)	1.935 (4)	Fe(4)–C(16)	1.927 (4)
Fe(1)–C(2)	1.756 (4)	Fe(3)–C(17)	1.769 (4)
Fe(2)–C(3)	1.751 (4)	Fe(4)–C(18)	1.764 (4)
Fe(1)–C(4)	1.968 (3)	Fe(3)–C(10)	1.963 (4)
Fe(2)–C(4)	1.985 (3)	Fe(4)–C(19)	1.984 (4)
C(1)–O(1)	1.180 (5)	C(16)–O(16)	1.176 (5)
C(2)–O(2)	1.146 (5)	C(17)–O(17)	1.135 (5)
C(3)–O(3)	1.148 (5)	C(18)–O(18)	1.143 (5)
C(4)–C(5)	1.449 (5)	C(19)–C(20)	1.464 (5)
C(5)–O(4)	1.214 (5)	C(20)–O(19)	1.206 (5)
C(4)–H(1)	1.00 (4)	C(19)–H(3)	1.01 (3)
C(5)–H(2)	1.05 (4)	C(20)–H(4)	1.07 (3)
		Mean Fe–C_{cp} Distance and Occupancies	
Fe(1)–C(6–10)A	2.12 (1) (0.58)	Fe(3)–C(21–25)A	2.12 (1) (0.82)
Fe(1)–C(6–10)B	2.13 (1) (0.42)	Fe(3)–C(21–25)B	2.15 (1) (0.18)
Fe(2)–C(11–15)A	2.13 (1) (0.62)	Fe(4)–C(26–26)A	2.13 (1) (0.65)
Fe(2)–C(11–15)B	2.13 (1) (0.38)	Fe(4)–C(26–30)B	2.13 (1) (0.35)
		Angles	
Fe(1)–C(1)–O(1)	140.0 (3)	Fe(3)–C(16)–O(16)	139.0 (3)
Fe(2)–C(1)–O(1)	137.7 (3)	Fe(4)–C(16)–O(16)	138.7 (3)
Fe(1)–C(2)–O(2)	174.6 (3)	Fe(3)–C(17)–O(17)	175.4 (4)
Fe(2)–C(3)–O(3)	175.5 (4)	Fe(4)–C(18)–O(18)	174.4 (4)
Fe(1)–C(4)–Fe(2)	79.5 (1)	Fe(3)–C(19)–Fe(4)	79.5 (1)
Fe(1)–C(4)–C(5)	121.5 (2)	Fe(3)–C(19)–C(20)	123.8 (3)
Fe(2)–C(4)–C(5)	116.6 (3)	Fe(4)–C(19)–C(20)	117.0 (3)
C(4)–C(5)–O(4)	125.3 (4)	C(19)–C(20)–O(19)	123.7 (4)
C(4)–C(5)–H(2)	120 (2)	C(19)–C(20)–H(4)	117 (3)
C(5)–C(4)–H(1)	106 (2)	C(20)–C(19)–H(3)	111 (3)

the generated formyl to the μ-carbyne carbon and bond formation between the sulfur atom and the coordinatively unsaturated Fe atoms ending up in the aldehydo complex **2** (eq 1).

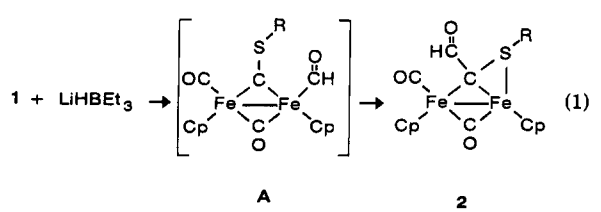

(1)

Since the formation of type **2** complexes is immediate and no metal–formyl intermediates could be spectroscopically detected, it is reasonable to assume that the thermodynamically favored **A** → **2** step, in which Fe–C bond-breaking is accompanied by Fe–S and C–C bond formation, is fast enough to prevent alternative decomposition routes including the irreversible decarbonylation which usually dominates the metal–formyl transformation. However, few examples of rearrangement reactions involving intramolecular CHO migrations are known.[13]

(13) (a) Heat, P. C.; Patton, A. T.; Gladysz, J. A. *J. Am. Chem. Soc.* **1986**, *108*, 1185. (b) Casey, C. P.; Palermo, R. E. *J. Am. Chem. Soc.* **1986**, *108*, 549. (c) Milletti, M. C.; Fenske, R. F. *Organometallics* **1989**, *8*, 420.

While these considerations provide a possible explanation for the formation of **2**, it is still not clear why the aldehydo complex $Fe_2[\mu\text{-}C(CHO)H](\mu\text{-}CO)(CO)_2(Cp)_2$ (**3**) is obtained as a byproduct from the reaction of **1** with $LiHBEt_3$. Since **3** has been originally prepared[7] from $[Fe_2\{\mu\text{-}C(CO)H\}(\mu\text{-}CO)(CO)_2(Cp)_2]^+$ and $[FeH(CO)_4]^-$, it should be hypothesized that its formation also occurs via the same μ-acylium complex. Independently of the mechanism, it is clear that the hydride cleavage of the C–S bond in **1** must occur at some stage of the reaction. This is relevant since nucleophilic cleavage of the μ-C–S bond in **1** has been observed only in the reactions with NCO^- and NHR_2, which afford $Fe_2[\mu\text{-}CNC(O)SR](\mu\text{-}CO)(CO)_2(Cp)_2$[3] and $Fe_2(\mu\text{-}CNR_2)(\mu\text{-}CO)(SR)(CO)(Cp)_2$,[1] respectively.

The complete sequence described by eq 1 is strongly supported by the reaction of **1** with RO^- resulting in the formation of $[Fe_2(\mu\text{-}CSR)(\mu\text{-}CO)(CO)(COOR)(Cp)_2]$ (**4**), which is the stable alkoxy-substituted counterpart of **A**. Type **4** complexes slowly decompose in CH_2Cl_2 solution to generate the esters $Fe\overline{Fe[\mu\text{-}C(COOR)SR]}(\mu\text{-}CO)(CO)(Cp)_2$ (**5**), via COOR migration to the bridging carbyne carbon. The observed stereogeometries of both **2b** and **5a** derivatives do not give simple clues to the sequence of intramolecular rearrangements that take place after the nucleophilic attack on the CO ligands. In the light of the demonstrated cis geometry of complex **1**, it is evident that the supposed migration of the CHO or C(O)OR group to the bridging carbyne carbon and the formation of the Fe–S bond cannot take place in a simple concerted way. In fact the transferred groups do not remain in the region of space occupied before migration, thus implying intermediate assembling in which bridge opening and ligand rotation can occur.

Despite the higher stability of the metal–alkoxycarbonyls compared to metal–formyls, the intramolecular rearrangement is accompanied by extensive decomposition. It is of interest to note that other dinuclear complexes containing a μ-C(R′)COOR group have been similarly generated by reacting the cationic alkylidynes $[MPt(\mu\text{-}CPh)(CO)_4(PMe_3)_3]^+$ (M = Cr, W) with alkoxides (MeO^-, EtO^-).[14] Our ability in preparing compounds **4** indicates that these reactions also occur via analogous dinuclear alkoxy–carbonyl intermediates, which must be regarded as very reactive species. A simple electron count on $[Fe_2(\mu\text{-}CSR)(\mu\text{-}CO)(COOR)(CO)(Cp)_2]$ (**4**) suggests that the bond between the μ-thiocarbyne carbon and the Fe atom bearing the COOR group should be stronger than in the parent species. This situation should allow a closer C(carbyne)–C(carboxy) contact and facilitate the migration of the COOR group. At this point, the reactivity of compounds **4** and their potential use in the organometallic synthesis have not been fully investigated. However, it is worthwhile mentioning that we have performed the reaction of **4a** with $Co_2(CO)_8$ in THF solution at room temperature, obtaining the trinuclear cluster $CoFe_2(\mu_3\text{-}CSMe)(CO)_5(Cp)_2$ (**6**) in about 33% yield. Complex **6** has been identified by comparison of its spectroscopic properties with those reported for the same complex previously prepared by reacting $NaCo(CO)_4$ with **1a** under photolysis.[4]

The results of the reaction of **1** with X^- (X = H, OR), far from providing an exhaustive description of the reaction mechanisms, simply underline their main aspects consisting in the C–X and C–C bond formation which involves both the terminally coordinated carbonyl and μ-alkylidyne groups. These are the key steps in the Fischer–Tropsch (FT) synthesis; therefore, the formation of type **2** and **5** derivatives may represent a model reaction for the catalytic process. In this direction our findings fit well with the mechanism[15] proposed by Keim to explain the formation of oxygenated species in the FT synthesis. The mechanistic interpretation has been suggested by observing the analogous reactions of $Fe_2(\mu\text{-}CH_2)(CO)_8$ with $KHB[CH(CH_3)C_2H_5]_3$ or methoxide, which form, via nucleophilic attack at the CO and subsequent coupling with the CH_2 bridging ligand, the unstable polynuclear metalated aldehyde $[Fe_n(CO)_mCH_2CHO]^-$ or acetate $[Fe_n(CO)_mCH_2COOCH_3]^-$, respectively.[16]

Experimental Section

General Procedures. All the solvents were appropriately dried and degassed prior to use under dinitrogen, and reactions were routinely carried out using standard Schlenk techniques under dinitrogen. All reagent grade chemicals were used as received. Column chromatography has been performed on alumina (Carlo Erba, neutral, activity grade III). The compounds $[Fe_2(\mu\text{-}CSR)(\mu\text{-}CO)(CO)_2(Cp)_2]SO_3CF_3$ (**1a,b**) were prepared by the reported procedures.[5] Infrared spectra were recorded on a Perkin-Elmer 983-G spectrometer in solution using a pair of matched 1.0-mm NaCl cells. ^1H and $^{13}C\{^1H\}$ NMR spectra were recorded, at room temperature, on a Varian XL 100 spectrometer using $SiMe_4$ as an internal standard; $[Cr(acac)_3]$ (acac = acetylacetonate) (0.1 mol L^{-1}) was added to the ^{13}C samples to reduce data collection time. Elemental analyses were determined by Pascher Microanalytical Laboratorium (Bonn, Germany). Melting points were uncorrected.

Preparation of $Fe\overline{Fe[\mu\text{-}C(CHO)SMe]}(\mu\text{-}CO)(CO)(Cp)_2$ (2a). A tetrahydrofuran solution (20 mL) of **1a** (0.48 g, 0.90 mmol) was cooled to −60 °C and treated with $LiHBEt_3$ (1.00 mL, 1 mol L^{-1} in THF). The solution was stirred for 15 min, and then the solvent was removed in vacuo and the residue was chromatographed on an alumina column (4 × 10 cm). Elution with a CH_2Cl_2–hexanes mixture (1:1) gave first a red band containing small amounts of the complex $[Fe(CO)_2(Cp)]_2$ (0.02 g). A second green band was collected and evaporated to dryness. The residual solid was dissolved in CH_2Cl_2, layered with *n*-pentane, and cooled to −20 °C affording dark-green crystals of **2a** (0.23 g, 67%), mp 145–147 °C dec. Anal. Calcd for $C_{15}H_{14}Fe_2O_3S$: C, 46.67; H, 3.65. Found: C, 46.80; H, 3.24. IR (CH_2Cl_2): ν(CO) 1958 s, 1782 ms, 1619 m cm^{-1}. ^1H NMR ($CDCl_3$): δ 11.7 (s, 1 H, CHO), 4.73 and 4.66 (s, 10 H, Cp), 1.73 (s, 3 H, SMe). ^{13}C NMR (CD_2Cl_2): 266.5 (μ-CO), 216.6 (CO), 199.9 (CHO), 161.7 (μ-C), 83.7, 82.8 (Cp), 27.0 (SMe). A third red fraction was collected, dried under vacuum, and recrystallized from a CH_2Cl_2–pentane mixture affording red crystals of the complex $Fe_2[\mu\text{-}C(H)CHO](\mu\text{-}CO)(CO)_2(Cp)_2$ (0.02 g, 6%).

Preparation of $Fe\overline{Fe[\mu\text{-}C(CHO)SEt]}(\mu\text{-}CO)(CO)(Cp)_2$ (2b). The synthesis of **2b** was carried out as described for **2a** by starting with $[Fe_2(\mu\text{-}CSEt)(\mu\text{-}CO)(CO)_2(Cp)_2]SO_3CF_3$ (**1b**) (0.55 g, 1.0 mmol): yield 0.25 g, 62%; mp 119–121 °C dec. Anal. Calcd for $C_{16}H_{16}Fe_2O_3S$: C, 48.03; H, 4.03. Found: C, 47.96; H, 4.05. IR (CH_2Cl_2): ν(CO) 1957 s, 1779 ms, 1620 m cm^{-1}. ^1H NMR (CD_2Cl_2): δ 11.49 (s, 1 H, CHO), 4.73 and 4.64 (s, 10 H, Cp), 2.60 (m, 1 H, SCH_2CH_3), 1.52 (m, 1 H, SCH_2CH_3), 1.11 (t, J = 7.5 Hz, 3 H, CH_2CH_3). ^{13}C NMR (CD_2Cl_2): δ 267.5 (μ-CO), 215.4 (CO), 200.7 (CHO), 162.9 (μ-C), 84.0, 83.0 (Cp), 38.7 (SCH_2CH_3), 14.7 (SCH_2CH_3).

(14) Howard, J. A. K.; Jeffery, J. C.; Laguna, M.; Navarro, R.; Stone, F. G. A. *J. Chem. Soc., Dalton Trans.* **1981**, 751.

(15) Hackenbruch, J.; Keim, W.; Roper, M.; Strutz, H. *J. Mol. Catal.* **1984**, *26*, 129.

(16) Keim, W.; Roper, M.; Strutz, H.; Kruger, C. *Angew. Chem., Int. Ed. Engl.* **1984**, *23*, 432.

Table IV. Relevant Bond Lengths (Å) and Angles (deg) for 5a

	molecule 1	molecule 2
Fe(1)–Fe(2)	2.500 (1)	2.540 (1)
Fe(1)–S	2.269 (1)	2.268 (1)
S–C(2)	1.777 (5)	1.771 (5)
S–C(1)	1.814 (6)	1.817 (6)
C(2)–C(3)	1.474 (7)	1.491 (7)
C(3)–O(1)	1.224 (7)	1.203 (7)
C(3)–O(2)	1.336 (7)	1.347 (6)
O(2)–C(4)	1.44 (1)	1.46 (1)
Fe(1)–C(5)	1.828 (5)	1.815 (5)
Fe(2)–C(5)	1.967 (6)	2.110 (5)
C(5)–O(5)	1.22 (1)	1.17 (1)
Fe(2)–C(6)	1.741 (5)	1.752 (6)
C(6)–O(6)	1.17 (1)	1.15 (1)
Fe(1)–C(10)	2.071 (4)	2.065 (4)
Fe(1)–C(11)	2.088 (5)	2.095 (5)
Fe(1)–C(12)	2.116 (5)	2.122 (5)
Fe(1)–C(13)	2.115 (5)	2.109 (4)
Fe(1)–C(14)	2.088 (4)	2.073 (4)
Fe(2)–C(15)	2.134 (5)	2.104 (4)
Fe(2)–C(16)	2.159 (5)	2.080 (4)
Fe(2)–C(17)	2.137 (5)	2.073 (4)
Fe(2)–C(18)	2.098 (5)	2.093 (4)
Fe(2)–C(19)	2.096 (5)	2.112 (4)
Fe(1)–C(2)	1.910 (5)	1.889 (5)
Fe(2)–C(2)	1.959 (5)	1.969 (5)
Fe(2)–Fe(1)–S	79.2 (1)	79.1 (1)
Fe(1)–S–C(1)	109.3 (2)	109.5 (2)
Fe(1)–S–C(2)	54.7 (2)	54.1 (2)
S–C(2)–C(3)	121.2 (3)	121.4 (3)
C(2)–C(3)–O(1)	125.1 (5)	124.5 (5)
O(1)–C(3)–O(2)	121.8 (5)	121.7 (5)
C(3)–O(2)–C(4)	117.4 (5)	115.7 (5)

Table V. Fractional Atomic Coordinates for 2b

atom	x	y	z
Fe(1)	0.17181 (2)	0.20192 (2)	0.97661 (1)
Fe(2)	0.35003 (2)	0.17260 (2)	0.88619 (1)
S	0.30383 (3)	–0.05246 (3)	0.91012 (2)
C(1)	0.37190 (15)	0.22760 (17)	0.99821 (9)
O(1)	0.44492 (14)	0.27485 (18)	1.05601 (9)
C(2)	0.19940 (16)	0.07059 (16)	1.05340 (9)
O(2)	0.2128 (2)	–0.0091 (2)	1.1080 (1)
C(3)	0.1842 (1)	0.0789 (2)	0.8804 (1)
O(3)	0.0256 (2)	–0.0477 (2)	0.7826 (1)
C(4)	0.0747 (2)	0.0609 (2)	0.8097 (1)
C(5)	0.3161 (2)	–0.1535 (2)	0.8154 (1)
C(6)	0.2511 (2)	–0.2948 (2)	0.8199 (1)
C(7)	–0.0157 (2)	0.2932 (2)	0.9259 (1)
C(8)	–0.0101 (2)	0.2569 (2)	1.0112 (2)
C(9)	0.0931 (2)	0.3314 (2)	1.0592 (1)
C(10)	0.1541 (2)	0.4125 (2)	1.0028 (2)
C(11)	0.0861 (2)	0.3868 (2)	0.9198 (1)
C(12)	0.3380 (2)	0.3188 (2)	0.7885 (1)
C(13)	0.4365 (2)	0.3568 (2)	0.8577 (1)
C(14)	0.5358 (2)	0.2520 (2)	0.8698 (1)
C(15)	0.4964 (2)	0.1483 (2)	0.8090 (1)
C(16)	0.3763 (2)	0.1904 (2)	0.7583 (1)

Preparation of $Fe_2(\mu\text{-CSMe})(\mu\text{-CO})(COOMe)(CO)(Cp)_2$ (4a). Sodium methoxide (2.24 mL, 0.5 mol L^{-1} solution in methanol) was added to a solution of **1a** (0.60 g, 1.12 mmol) in THF (30 mL) at −20 °C. The mixture was stirred for 10 min, allowed to warm at room temperature, and filtered through a Celite pad. The volatile material was removed in vacuo, and the residue was recrystallized from a CH_2Cl_2–*n*-pentane mixture affording dark green crystals of **4a** (0.30 g, 65%), mp 95–97 °C dec. Anal. Calcd for $C_{16}H_{16}Fe_2O_4S$: C, 46.19; H, 3.88. Found: C, 46.26; H, 4.21. IR (CH_2Cl_2): ν(CO) 1984 s, 1805 s, 1614 m cm^{-1}. ^1H NMR ($CDCl_3$): δ 4.81 and 4.79 (s, 10 H, Cp), 3.41 (s, 3 H, SMe), 3.01 (s, 3 H, OMe). ^{13}C NMR (CD_2Cl_2): δ 395.9 (μ-C), 265.1 (μ-CO), 213.1 (CO), 203.7 ($COOCH_3$), 89.1, 87.2 (Cp), 50.0 (OMe), 29.9 (SMe).

The following $[Fe_2(\mu\text{-CSR})(\mu\text{-CO})(CO)(COOR')(Cp)_2]$ complexes were obtained by analogous procedures.

Table VI. Fractional Atomic Coordinates for 3

atom	x	y	z
Fe(1)	0.65852 (5)	0.01383 (3)	0.19363 (3)
Fe(2)	0.39806 (5)	0.06065 (3)	0.19236 (3)
Fe(3)	–0.16301 (5)	0.18080 (3)	0.50297 (3)
Fe(4)	0.09665 (5)	0.20626 (3)	0.46157 (3)
C(1)	0.5329 (4)	0.0397 (2)	0.2797 (2)
O(1)	0.5321 (3)	0.0404 (2)	0.3505 (1)
C(2)	0.7575 (4)	0.0961 (2)	0.2103 (2)
O(2)	0.8301 (3)	0.1465 (2)	0.2244 (2)
C(3)	0.4214 (4)	0.1557 (2)	0.2111 (2)
O(3)	0.4279 (4)	0.2179 (2)	0.2259 (2)
C(4)	0.5404 (4)	0.0531 (2)	0.1037 (2)
C(5)	0.5786 (4)	0.1218 (2)	0.0637 (2)
O(4)	0.5631 (3)	0.1339 (2)	–0.0075 (2)
C(16)	0.0364 (4)	0.1274 (2)	0.4327 (2)
O(16)	–0.0362 (3)	0.0721 (1)	0.3952 (2)
C(17)	–0.2601 (4)	0.2161 (2)	0.4189 (2)
O(17)	0.3292 (3)	0.2351 (2)	0.3657 (2)
C(18)	0.0684 (4)	0.2435 (2)	0.3647 (2)
O(18)	0.0596 (4)	0.2642 (2)	0.3000 (2)
C(19)	0.0453 (4)	0.2712 (2)	0.5171 (2)
C(20)	–0.0802 (4)	0.3424 (2)	0.4790 (2)
O(19)	–0.0680 (4)	0.4016 (2)	0.5124 (2)
C(A6)	0.6278 (4)	0.1043 (3)	0.1859 (3)
C(A7)	0.7089 (4)	–0.0848 (3)	0.2560 (3)
C(A8)	0.8385 (4)	–0.0482 (3)	0.2315 (3)
C(A9)	0.8375 (4)	0.0450 (3)	0.1464 (3)
C(A10)	0.7072 (4)	–0.0709 (3)	0.1182 (3)
C(B6)	0.6628 (7)	–0.0953 (4)	0.2463 (3)
C(B7)	0.8000 (7)	–0.0594 (4)	0.2563 (3)
C(B8)	0.8555 (7)	–0.0439 (4)	0.1788 (3)
C(B9)	0.7526 (7)	–0.0702 (4)	0.1211 (3)
C(B10)	0.6334 (7)	–0.1020 (4)	0.1628 (3)
C(A11)	0.2687 (6)	–0.0274 (3)	0.2374 (3)
C(A12)	0.1994 (6)	0.0421 (3)	0.2510 (3)
C(A13)	0.1702 (6)	0.0754 (3)	0.1753 (3)
C(A14)	0.2215 (6)	0.0266 (3)	0.1149 (3)
C(A15)	0.2823 (6)	–0.0369 (3)	0.1532 (3)
C(B11)	0.2267 (10)	0.0115 (6)	0.2617 (3)
C(B12)	0.1737 (10)	0.0736 (6)	0.2174 (3)
C(B13)	0.1923 (10)	0.0583 (6)	0.1346 (3)
C(B14)	0.2568 (10)	–0.0132 (6)	0.1276 (3)
C(B15)	0.2780 (10)	–0.0421 (6)	0.2062 (3)
C(A21)	–0.1829 (4)	0.0782 (2)	0.5632 (2)
C(A22)	–0.3216 (4)	0.1023 (2)	0.5343 (2)
C(A23)	–0.3544 (4)	0.1711 (2)	0.5718 (2)
C(A24)	–0.2359 (4)	0.1895 (2)	0.6239 (2)
C(A25)	–0.1299 (4)	0.1320 (2)	0.6186 (2)
C(B21)	–0.1396 (16)	0.0860 (8)	0.5853 (12)
C(B22)	–0.2725 (16)	0.0806 (8)	0.5408 (12)
C(B23)	–0.3578 (16)	0.1445 (8)	0.5578 (12)
C(B24)	–0.2775 (16)	0.1894 (8)	0.6128 (12)
C(B25)	–0.1427 (16)	0.1533 (8)	0.6298 (12)
C(A26)	0.2329 (6)	0.1276 (2)	0.5203 (3)
C(A27)	0.2973 (6)	0.1507 (2)	0.4473 (3)
C(A28)	0.3236 (6)	0.2284 (2)	0.4524 (3)
C(A29)	0.2754 (6)	0.2532 (2)	0.5285 (3)
C(A30)	0.2194 (6)	0.1909 (2)	0.5705 (3)
C(B26)	0.2788 (11)	0.1293 (3)	0.4620 (4)
C(B27)	0.3227 (11)	0.2021 (3)	0.4400 (4)
C(B28)	0.2921 (11)	0.2504 (3)	0.5051 (4)
C(B29)	0.2292 (11)	0.2074 (3)	0.5672 (4)
C(B30)	0.2210 (11)	0.1326 (3)	0.5406 (4)

$Fe_2(\mu\text{-CSMe})(\mu\text{-CO})(CO)(COOEt)(Cp)_2$ (4b): yield 59%; mp 83–85 °C dec. Anal. Calcd for $C_{17}H_{18}Fe_2O_4S$: C, 47.47; H, 4.22. Found: C, 47.85; H, 4.18. IR (CH_2Cl_2): ν(CO) 1983 s, 1803 s, 1607 m cm^{-1}. ^1H NMR ($CDCl_3$): δ 4.84 and 4.81 (s, 10 H, Cp), 3.52 (q br, 2 H, OCH_2CH_3), 3.43 (s, 3 H, SMe), 0.90 (t, 3 H, OCH_2CH_3).

$Fe_2(\mu\text{-CSEt})(\mu\text{-CO})(COOEt)(CO)(Cp)_2$ (4c): yield 70%; mp 109–111 °C dec. Anal. Calcd for $C_{18}H_{20}Fe_2O_4S$: C, 48.68; H, 4.54. Found: C, 48.59; H, 4.61. IR (CH_2Cl_2): ν(CO) 1983 s, 1804 s, 1607 m cm^{-1}. ^1H NMR ($CDCl_3$): δ 4.84 and 4.82 (s, 10 H, Cp), 4.02 (q br, 2 H, OCH_2CH_3), 3.54 (q, J = 8.0 Hz, 2 H, SCH_2CH_3), 1.55 (t, 3 H, SCH_2CH_3), 0.91 (t, 3 H, OCH_2CH_3).

Table VII. Fractional Atomic Coordinates for 5a

atom	x	y	z
Fe(1A)	0.07571 (4)	0.55545	0.36783 (3)
Fe(2A)	0.09181 (5)	0.75412 (8)	0.43498 (3)
S(1A)	0.23438 (8)	0.59087 (14)	0.36968 (5)
C(1A)	0.2914 (4)	0.3977 (7)	0.3519 (2)
C(2A)	0.1619 (3)	0.5505 (6)	0.4191 (2)
C(3A)	0.1849 (4)	0.4157 (6)	0.4525 (2)
O(1A)	0.1270 (3)	0.3297 (5)	0.4733 (2)
O(2A)	0.2774 (3)	0.4003 (5)	0.4602 (1)
C(4A)	0.3070 (6)	0.2770 (9)	0.4940 (3)
C(5A)	0.0501 (4)	0.7797 (7)	0.3697 (2)
O(5A)	0.0136 (3)	0.8957 (5)	0.3486 (1)
C(6A)	0.1822 (4)	0.8928 (7)	0.4209 (2)
O(6A)	0.2382 (3)	0.9960 (6)	0.4123 (2)
C(10A)	−0.0617 (3)	0.5109 (6)	0.3467 (2)
C(11A)	−0.002 (3)	0.4910 (6)	0.3079 (2)
C(12A)	0.0637 (3)	0.3593 (6)	0.3184 (2)
C(13A)	0.0417 (3)	0.2979 (6)	0.3637 (2)
C(14A)	−0.0358 (3)	0.3916 (6)	0.3812 (2)
C(15A)	−0.0169 (4)	0.6535 (5)	0.4782 (2)
C(16A)	0.0635 (4)	0.6840 (5)	0.5066 (2)
C(17A)	0.0850 (4)	0.8575 (5)	0.5039 (2)
C(18A)	0.0178 (4)	0.9341 (5)	0.4739 (2)
C(19A)	−0.0451 (4)	0.8080 (5)	0.4580 (2)
Fe(1B)	0.32931 (4)	−0.44225 (7)	0.71154 (3)
Fe(2B)	0.34560 (4)	−0.24277 (8)	0.64276 (3)
S(1B)	0.48781 (8)	−0.40582 (14)	0.70961 (5)
C(1B)	0.5459 (4)	−0.5999 (7)	0.7261 (2)
C(2B)	0.4145 (3)	−0.4469 (6)	0.6608 (2)
C(3B)	0.4379 (4)	−0.5814 (6)	0.6265 (2)
O(1B)	0.3806 (3)	−0.6672 (5)	0.6068 (1)
O(2B)	0.5309 (3)	−0.5964 (5)	0.6179 (1)
C(4B)	0.5568 (5)	−0.7200 (9)	0.5827 (2)
C(5B)	0.2988 (3)	−0.2215 (6)	0.7126 (2)
O(5B)	0.2671 (3)	−0.1032 (5)	0.7308 (1)
C(6B)	0.4341 (4)	−0.1030 (7)	0.6602 (2)
O(6B)	0.4888 (3)	−0.0016 (6)	0.6691 (2)
C(10B)	0.1923 (3)	−0.4837 (5)	0.7329 (2)
C(11B)	0.2534 (3)	−0.5071 (5)	0.7718 (2)
C(12B)	0.3162 (3)	−0.6399 (5)	0.7608 (2)
C(13B)	0.2940 (3)	−0.6985 (5)	0.7152 (2)
C(14B)	0.2174 (3)	−0.6020 (5)	0.6980 (2)
C(15B)	0.2468 (3)	−0.3514 (5)	0.5970 (1)
C(16B)	0.3249 (3)	−0.2864 (5)	0.5717 (1)
C(17B)	0.3301 (3)	−0.1116 (5)	0.5806 (1)
C(18B)	0.2552 (3)	−0.0686 (5)	0.6113 (1)
C(19B)	0.2038 (3)	−0.2168 (5)	0.6215 (1)

Preparation of $FeFe[\mu$-C(COOMe)SMe$](\mu$-CO)(CO)$(Cp)_2$ (5a). The compound **4a** (0.25 g, 0.60 mmol) was stirred in dichloromethane (20 mL) for about 6 h at room temperature. The solvent was then removed in vacuo, and the residue was chromatographed on an alumina column (3 × 15 cm). Elution with a CH_2Cl_2–hexanes mixture (1:2) gave first a red-brownish fraction containing $Fe_2(\mu$-CS$)(\mu$-CO$)(CO)_2(Cp)_2$ and $[Fe(\mu$-CO$)$(CO)(Cp)$]_2$. A second green fraction was collected and evaporated to dryness under high vacuum. Recrystallization of the residual solid afforded dark-green crystals of **5a** (0.05 g, 22%), mp 165–167 °C dec. Anal. Calcd for $C_{16}H_{16}Fe_2O_4S$: C, 46.19; H, 3.88. Found: C, 46.31; H, 3.70. IR (CH_2Cl_2): ν(CO) 1949 s, 1775 s, 1675 m cm^{-1}. ^{1}H NMR ($CDCl_3$): δ 4.59 (s br, 10 H, Cp), 4.06 (s, 3 H, OMe), 1.57 (s, 3 H, SMe).

The following $FeFe[\mu$-C(COOR′)SR$](\mu$-CO)(CO)$(Cp)_2$ complexes were obtained by analogous procedures.

$FeFe[\mu$-C(COOEt)SMe$](\mu$-CO)(CO)$(Cp)_2$ (5b): yield 34%; mp 157–160 °C dec. Anal. Calcd for $C_{17}H_{18}Fe_2O_4S$: C, 47.47; H, 4.22. Found: C, 47.13, H, 4.38. IR (CH_2Cl_2): ν(CO) 1949 s, 1773 s, 1671 m cm^{-1}. ^{1}H NMR ($CDCl_3$): δ 4.40 (s br, 10 H, Cp), 4.43 (q, 2 H, CH_2CH_3), 1.24 (t, 3 H, CH_2CH_3), 1.10 (s, 3 H, SMe). ^{13}C NMR (CD_2Cl_2): δ 245.2 (μ-CO), 217.1 (CO), 180.0 (COOEt), 155.7 (μ-C), 85.7, 83.8 (Cp), 61.2 (OCH_2CH_3), 28.5 (SCH_3), 15.1 (OCH_2CH_3).

$FeFe[\mu$-C(COOEt)SEt$](\mu$-CO)(CO)$(Cp)_2$ (5c): yield 9%; mp 116–118 °C dec. Anal. Calcd for $C_{18}H_{20}Fe_2O_4S$: C, 48.68; H, 4.54. Found: C, 48.76; H, 4.64. IR (CH_2Cl_2): ν(CO) 1949 s, 1773 s, 1672 m cm^{-1}.

X-ray Structure Determination of 2b, 3, and 5a. Crystal data and details of the measurements for the three data collections are summarized in Table I. Diffraction intensities were collected at room temperature on an Enraf-Nonius CAD-4 diffractometer equipped with Mo Kα radiation and reduced to F_o values; no decay correction was necessary. The structures were solved by direct methods, which afforded the position of the Fe atoms; all remaining atoms were located by subsequent difference Fourier syntheses. The unit cells of both **3** and **5a** were found to contain two independent, but chemically equivalent, molecules (**A** and **B** in Tables III and IV). The cyclopentadienyl rings in **3** were affected by rotational disorder, very likely arising from the presence of a double-well potential for ring reorientation in the solid state. Partial occupancies were refined for the four pairs of disordered images (see Table III). All cyclopentadienyl and aliphatic hydrogen atoms were added in calculated positions (C–H = 1.08 Å), while the chemically more significant H(carbene) and H(formyl) atoms in **3** could be located directly from the Fourier syntheses. Their positions were refined by "constraining" the C–H distances to the observed values. The structural model refinements were carried out by least-squares calculations, the minimized function being $\sum w(|F_o|-K|F_d|)^2$. The weighting scheme employed was $w = K/[\sigma^2(F) + |g|F^2]$, where both K and g were refined. For all calculations the SHELX[17] package of crystallographic programs was used with the scattering factors, corrected for the real and imaginary parts of anomalous dispersion, taken from ref 18. All atoms were allowed to vibrate anisotropically, except the H atoms, which were treated by refining common isotropic U values for the H(ring) atoms. Fractional atomic coordinates for **2b**, **3**, and **5a** are reported in Tables V–VII.

Acknowledgment. We thank the CNR and Ministero della Università e Ricerca Scientifica (MURST) for financial support.

Supplementary Material Available: Tables of anisotropic thermal parameters, fractional atomic coordinates for the hydrogen atoms, and complete bonds and angles for **2b**, **3**, and **5a** (102 pages). Ordering information is given on any current masthead page.

OM920401Q

(17) Sheldrick, G. M. SHELX76, Program for Crystal Structure Determination. University of Cambridge, Cambridge, England, 1976.
(18) *International Tables for X-ray Crystallography*; Kynoch Press: Birmingham, England, 1975; Vol. IV, pp 99–149.